An Analysis of Preliminary Test Campaign Results for a Microscale Solar Thermal Engine

Major Fred Kennedy, U.S. Air Force
Surrey Space Centre
University of Surrey
Guildford, Surrey GU2 7XH
+44 (0) 1483 689278 (voice)
+44 (0) 1483 689503 (fax)
F.Kennedy@sstl.co.uk

Advisor: Dr. Phil Palmer, Reader
Surrey Space Centre
University of Surrey
Guildford, Surrey GU2 7XH
+44 (0) 1483 686024 (voice)
+44 (0) 1483 689503 (fax)
P.Palmer@sstl.co.uk

Abstract

In the fall of 2001, the author embarked on an investigation of small (< 100 kg) satellites augmented with high-performance solar thermal propulsion (STP). Small satellites have historically been confined to low earth orbits, with only a very limited capability to alter orbital parameters. A solar thermal propulsion system, properly downsized, could enable microsatellites to perform missions to high earth orbit, as well as lunar, near earth asteroid, and interplanetary intercepts, without the aid of expensive upper stages. Specific impulses of up to 400 seconds (s) are theoretically achievable, with storable monopropellants; velocity changes of up to 3,000 m/s may therefore be attained.

This paper will briefly review a selection of benchmark missions and their requirements, and the preliminary and detailed design choices including specific ground rules. However, the focus of the paper is on recent component test results in three key areas: (1) novel ceramic gasketing and metal-to-ceramic bonding methods, a necessity for hermetically sealing the solar thermal cavity receiver; (2) optical performance measurements of a lightweight metal solar concentrating mirror; and (3) thermal performance measurements of the insulated cavity receiver in a series of electrical heating tests in vacuum. A comparison of test data will be made to the results of the author's optical and thermal models, demonstrating strong agreement between predicted and actual results. These results strongly suggest that solar thermal propulsion can in fact provide substantial orbit transfer capability to small satellites.

Introduction

Microsatellites are enjoying a burgeoning reputation in the space industry, now taking on tasks and missions that were once the sole purview of much larger platforms. Revolutions in the development of micro-circuitry, software, and sensors has led to remarkably capable yet low-cost spacecraft; AlSAT, a Surrey Satellite Technologies, Ltd. (SSTL) satellite developed jointly with a team of Algerian scientists and launched in late 2002, carries multiple banks of 32-metre imaging cameras, gigabyte storage capacity, and S-band communications capability.[1] While these capabilities could theoretically be extended to missions in various orbits, including Geosynchronous Earth Orbit (GEO) and beyond, in practice this has not been the case. Constraints on mass, volume, and power have greatly limited both the available types and performance of small satellite propulsion systems (Fig. 1). Electric propulsion, while potentially offering very high specific impulse performance (1,000-10,000 s of I_{sp}), demands substantial power input; the roughly 100 W typically made available on a microsatellite platform is insufficient to provide more than a few tens of milliNewtons (mN) of thrust, driving orbit transfer times to months or years. Chemical propulsion systems are inherently limited by the reaction energy available—and are for the most part incapable of generating I_{sp} figures greater than about 300 s.

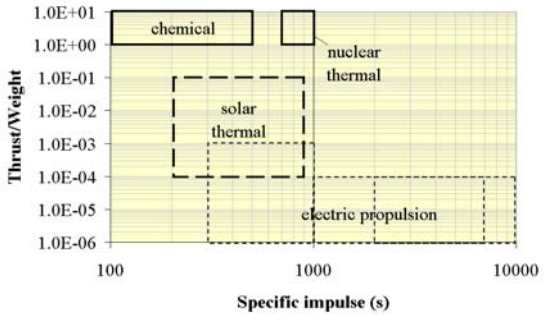

Figure 1. Performance of solar thermal propulsion systems vis-à-vis chemical, electric, and nuclear thermal propulsion options[2]

Over the past decade, research at the Surrey Space Centre has examined low-power resistojets, hybrid gas-solid motors, monopropellant, and bipropellant schemes,[3,4,5,6,7] partly in an effort to achieve a

low-cost, moderate-performance orbit transfer engine. In several recent publications, the author has demonstrated that a lightweight solar thermal engine, using storable monopropellants (e.g., water, ammonia, or hydrazine) and simplified subsystems, permit microsatellites to achieve on-orbit velocity changes on the order of 1,500-3,000 m/s. Adding substantial propulsive capability to microsatellites has the potential to dramatically increase their utility—extending their range to GEO, lunar missions, and beyond (Fig. 2). Using only moderate thrust (500-5,000 mN) firings of the solar thermal engine at or near apsidal crossings, orbital transfers from elliptical Geosynchronous Transfer Orbits (GTOs) to GEO can be accomplished in only a month. Similar transfers to the Moon and Near Earth Objects (NEOs) would require 150-300 days.[8]

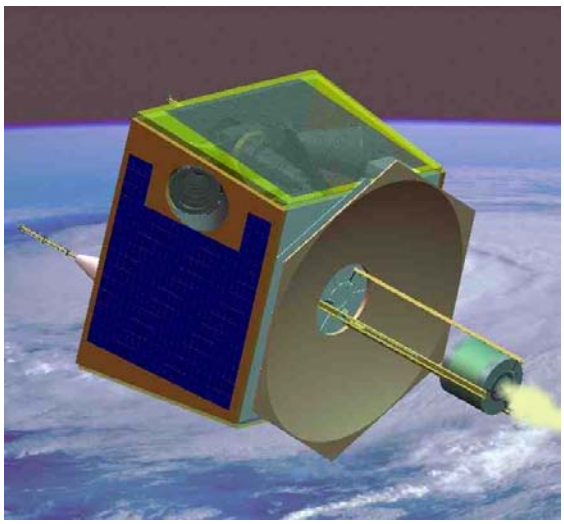

Figure 2. 3,000 mN thrust solar thermal propulsion system hosted aboard notional SSTL 100-kg microsatellite. Peak I_{sp} = 400 s.

The solar thermal propulsion system under development at the Surrey Space Centre relies on collected, highly concentrated sunlight to heat a blackbody cavity receiver to temperatures of 2,000-2,500 K. Propellant is then passed through a bed of thermal storage material inside the receiver, and exhausted to provide thrust. The system is being built as a proto-qualification/proto-flight unit (i.e., tested to qualification levels and subsequently used in on-orbit operations). This will minimize the number of experimental iterations prior to flight and is expected to reduce overall development cost.

The testing program includes extensive thermal testing on the main engine subcomponent, the thermal storage receiver. This device, constructed from refractory ceramic composite materials, was produced after an extensive review of potential materials and subsequent high-temperature vacuum testing of the most likely candidates. The receiver structure was tested for joint hermiticity at ambient temperature, with further seal tests planned at high temperature *in vacuo*. No-flow electrical heating tests are underway; they will be followed later this summer by full-flow testing with inert gas and ammonia propellant.

Optical path testing was performed on the main mirror element, a parabolic on-axis metal mirror designed to mount to a microsatellite face. Key mirror attributes, including geometric concentration ratio and focal point flux, have been determined in a series of preliminary tests. Optical system sensitivity to tracking and focal length errors will be assessed and compared to theoretical results. Full optical path testing, to include the mirror and solar receiver elements, represents the next step in validating the design of the solar thermal engine. Either on-sun testing or simulated solar radiation will be used to ground-test the engine at the system level. Results of this final developmental test are expected in early 2004.

The intended result of this activity is a low-cost, fully qualified, flight-ready solar thermal engine, prepared for integration and launch aboard a microsatellite host, no later than 2005.

Missions, Requirements, and Design

The author examined a number of stressing candidate missions, including lunar orbiters (e.g., ESA's SMART-1, LunarSat), GEO missions (e.g, Surrey's proposed GeMINI), and Near Earth Object (NEO) probes, all with substantial delta-V (ΔV) requirements.[9,10,11,12] Three classes of microsatellite mission were found to benefit from the application of STP: (1) GEO insertion missions, (2) Near-Escape missions, and (3) Other Body (e.g., lunar) capture missions. Many of these missions can be accomplished for under 2,000 m/s, with flight times ranging from 35 days (to GEO) to several hundred days (for lunar capture and NEO flybys). The solar thermal propulsion system's key requirements were derived from critical mission parameters, resulting in an acceptable range of transfer times, thrust levels, system mass and volume, and I_{sp} (Table 1).

Three designs resulted from the requirements development process—a large (2,800 N-s impulse) engine, a small (750 N-s) engine, and a proof-of-concept engine capable of producing 400 N-s of impulse per orbit, sufficient for

modest orbit-raising. The author subsequently selected the smallest of these, designated the *Mk. I*, as a design point for component testing, under the assumption that a "first flight" engine will most likely be a simple demonstrator and will not provide ΔVs greater than several hundred m/s.

	Threshold	Objective
Enclosed volume	90 liters	45 liters
System Mass	15 kg	10 kg
Burn-averaged I_{sp}	350 s	400 s
Per-Burn Impulse	750 N-s (GTO-GEO)	
Thermal Charging Time	4 hr (GTO-GEO)	2 hr (GTO-GEO)

Table 1. Example performance parameters for a micro-scale solar thermal engine (100 kg host).

Inherent microsatellite constraints and cost drove the design. The use of storable propellants—as opposed to difficult-to-handle cryogens such as hydrogen—was mandated. This limits theoretical performance to roughly 400 s of I_{sp}. While hydrazine (N_2H_4) was selected as the primary propellant owing to its flight heritage, ammonia (NH_3) is a less toxic, less expensive alternative. Hydrazine's principal advantage over ammonia is its energetic decomposition, which "pre-heats" the propellant stream and allows a further downsizing of the cavity receiver. Also, hydrazine's density-I_{sp} (DI_{sp}) is substantially higher than ammonia's, providing a greater propellant load for a given microsatellite configuration. Water and methane were also researched as options, but each has specific problems (e.g., coking, corrosive high temperature behaviour) tending to obviate their use.

The choice of propellant dictates the selection of cavity structure and bed materials that can survive in high temperature nitrogen and hydrogen (Fig. 3). A number of potential materials were examined; the clear winner was boron nitride (BN) and its ceramic composite formulations. BN is notably inert in ammonia or decomposed hydrazine at temperatures exceeding 2,000 K. It is also easily machined and thermally shock resistant, possessing a high specific heat value (1,988 J/kg-K at 2,000 K) and high melting point (3,273 K). Its high porosity (14%) prevents its use in pure form; as a composite with other ceramics, nearly 100% density can be achieved. Graphite, refractory metals such as tungsten, molybdenum, or rhenium, and various other ceramics (e.g., BeO, Al_2O_3) were ruled out for a variety of reasons, including machining cost, incompatibility with propellants, and toxicity.

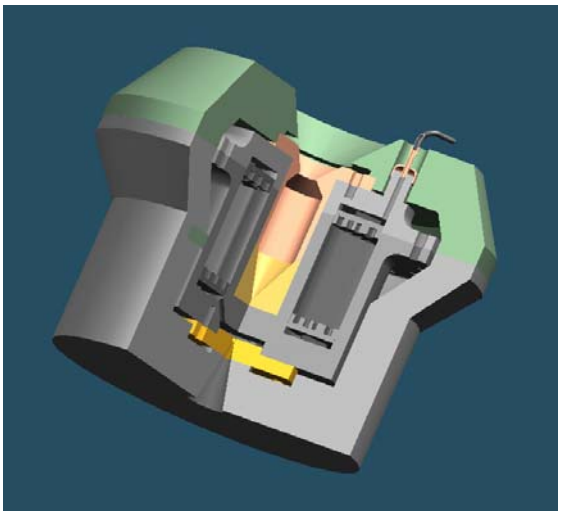

Figure 3. Mk. I cavity receiver solid model, 1.3 kg, BN particle bed in TiB_2/BN containment. Insulation package is 100% graphite foam.

Perhaps the most important and overarching design choice was the selection of a multi-impulse firing strategy over its alternative, the continuous firing (or spiral transfer) strategy. Given the prohibition on the use of hydrogen as a propellant, minimizing ΔV requirements becomes paramount; for a given set of transfer orbits, an impulsive firing strategy will always require a smaller velocity change than a spiral transfer.*

This choice cascades through the remaining design alternatives. For reasonable transfer times, substantial impulses have to be delivered at orbital apogee or perigee. This requires thrust levels of several hundred to several thousand mN for microsatellites. A "direct-gain" system, which transfers concentrated sunlight directly to the propellant, must provide this power input throughout the firing, which is likely to be as long as fifteen minutes at perigee. From:

$$P = \tfrac{1}{2}\, T g I_{sp},$$

we see that the jet power (P) required for a thrust level (T) of 3,000 mN and an Isp of 400 s is 5.9 kW. Assuming nominal reflectance (0.9) and pointing loss (0.9), this power level would require an articulating mirror with a diameter in excess of 2.6 m, an indisputably expensive

* The delta-V penalty associated with a spiral transfer from Low Earth Orbit (LEO) to GEO is approximately 40%, or nearly 2,000 m/s. This penalty is acceptable if the propulsion system's I_{sp} is sufficiently high—e.g., if electric propulsion is used.

item to produce. Furthermore, given microsatellite launch volume constraints,[†] such a mirror would have to be deployed after reaching initial orbit. The alternative to direct-gain is thermal storage, capturing incident sunlight and storing it as latent heat in an insulated receiver. This allows a much smaller mirror element, with the added advantage of decoupling sun-pointing from thrusting, permitting the use of rigid, fixed mirrors. A thermal storage engine can be thus "charged" for several hours and then fired in any conceivable direction. The problem of precise attitude control—crucial in a system that must track the sun to 0.1° accuracy—can be relegated to the microsatellite's onboard system.

A rigid, fixed 56-cm diameter aluminium concentrating mirror was selected from a range of alternatives (Fig. 4). With an expected output of 270 W and a concentration ratio in excess of 10,000:1, the mirror was predicted to be capable of heating the *Mk. I.* cavity receiver to temperatures in excess of 2,000 K. Other approaches, including inflatable and rigid deployable systems, were deemed unsuitable as a result of their higher complexity or lack of technical readiness. A rigid carbon fibre reinforced polymer (CFRP) mirror was regarded as a more flight-like, but significantly more expensive, alternative to the metal concentrator.

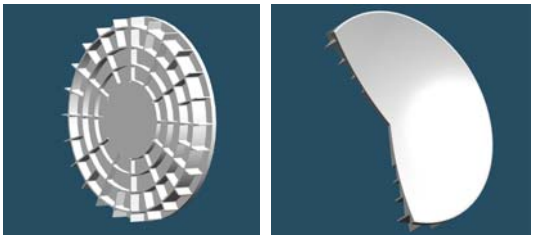

Figure 4. Mk. I solar concentrating mirror, lightweighted diamond-turned aluminium substrate, uncoated, f/.60 (rim angle = 45°).

Key figures of merit for solar concentrators include areal density (kg/m²) and root-mean-square (RMS) slope error. Traditional materials—to include glass and metals—typically cluster in the 50-75 kg/m² regime.[14] CFRP or composite mirrors hold the promise of 10 kg/m² or better; however, they are not yet capable of providing acceptable imaging performance at optical frequencies,[15] which raises the question of whether such mirrors are in fact viable as concentrators.[‡] Yet, as will be seen in the next section, it is possible to ascertain focal spot size and therefore concentration ratio on the basis of a mirror's known form error. This has led the author to conclude that state-of-the-art CFRP mirrors—which provide good imaging capability in the millimetre and submillimetre regime—should provide acceptable concentration.

The *Mk. I* engine's key components were manufactured during the winter of 2002-3, with preliminary testing commencing in early spring. The remainder of this paper is devoted to the results of this preliminary testing, and an initial assessment of the congruence between the testing and the author's ongoing STP modelling and simulation findings.

Preliminary Modelling and Test Results

Initial component testing of the solar thermal propulsion system has focused on three critical areas: high temperature material survivability, seal hermeticity, and bonding of selected ceramics and metals; thermal performance characteristics of the insulated solar receiver; and optical performance characteristics of the solar concentrating mirror. Test results were compared to the author's thermal and optical models, which include both in-house and commercial software packages.[§]

Material Survivability and Bonding Tests

The solar receiver must be capable of surviving repeated cycling between ambient (290 K) and peak operating temperatures of 2,000-2,500 K. It must also be capable of withstanding chemical attack from hot ammonia, hydrazine, or various decomposition products (e.g., N_2, H_2).

Two composite ceramics were selected for further consideration as receiver structural

[†] The Ariane Structure for Auxiliary Payloads (ASAP) constrains small satellites to a footprint of 60 x 60 cm.[13]

[‡] Designers of imaging systems often make use of RMS wavefront or form error to estimate the quality of their optics, since they wish to ensure that the wavefront arrives at the focal point in-phase. It is not at all clear that a poor wavefront error figure implies an unacceptable slope error; slope error is heavily dependent on a mirror's "microroughness," small-scale deviations from the "perfect" surface. If such imperfections can be reduced to the order of a wavelength of light (400-800 nanometres at optical frequencies) or less, they will have little effect on the mirror's ability to concentrate sunlight.

[§] Optical performance modelling was performed using OSLO LT 6.1, an optical ray-tracing package available as freeware from Sinclair Optics. Thermal modeling was performed using a combination of author-developed Visual Basic codes and Thermoanalytics, Inc., Wintherm 7.0.

materials: (1) Zirconia-Strengthed Boron Nitride (ZSBN), a blend of 45% zirconia (ZrO_2), 7% silicon carbide, and 48% boron nitride by weight; and (2) an Intermetallic Composite (IMC) of 46% titanium diboride (TiB_2) and 49% boron nitride. Both are low porosity ceramics with good machinability characteristics, high thermal shock resistance, low coefficients of thermal expansion (CTE), and high temperature strength.[16,17] IMC was retained as an alternative due to vendor concerns over possible chemical reactions in ZSBN at 2,300 K.

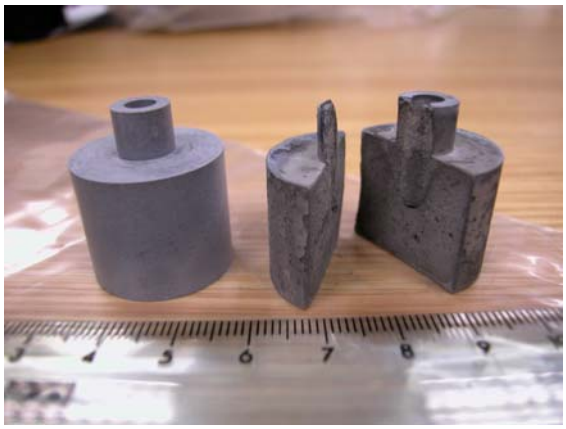

Figure 5. Pristine (left) and heated (right) samples of ZSBN ceramic composite, 40 minutes at 2,300 K, 20 mbar He environment, graphite furnace.

Several specimens of each material were exposed to temperatures of approximately 2,300 K for up to 40 minutes in a low-pressure He atmosphere (20 mbar). Figure 5 demonstrates the poor high-temperature performance of ZSBN—both tested samples lost in excess of 40% of their pre-test mass during their short exposure. One of the ZSBN elements fractured into two sections, displaying evidence of heating-induced vaporization and porosity. The IMC specimens performed significantly better; while they experienced some darkening due to surface graphitisation, they lost just 0.35% and 2.3% of their pre-test mass, respectively. Other than the single ZSBN fracture, neither set of samples suffered significant dimensional changes.

Both sets of samples produced a flaky white residue that precipitated out on various elements of the graphite furnace, which post-test X-Ray Photoelectron Spectroscopy (XPS) examination of the specimens revealed to be boric oxide (B_2O_3), a binder material present in small amounts in both ceramics. A dark residue precipitated out on the surface of the IMC elements, which was demonstrated to be elemental carbon. Based on these results, the author selected IMC as the primary receiver structural material for the component test phase.

Figure 6. Post-test samples of IMC ceramic composite, 40 minutes at 2,300 K, 20 mbar He environment, graphite furnace.

In addition to surviving at temperature in vacuum, the solar receiver must be capable of being assembled from a selection of subcomponents, with hermetic outer seals preventing the release of propellant gas into space. While metallic structures enjoy a variety of options for sealing, to include welding, mechanical bonding, and brazing, the nitride ceramics investigated by the author for use in a solar thermal engine are typically inert at high temperatures, sublime rather than melt, and are fairly brittle. While BN is notable in that its tensile strength rises considerably with temperature, its inertness makes it very difficult to bond to itself, other ceramics, or metals.[18,19] Its use in crucibles and metallizing boats attests to its lack of chemical reactivity, even at elevated temperatures.

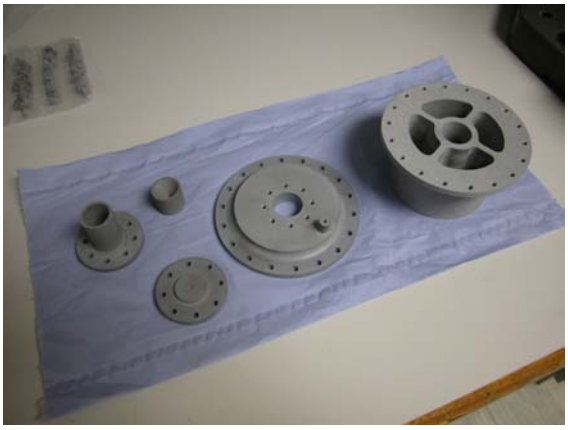

Figure 7. IMC (TiB_2/BN) solar receiver subcomponents, disassembled.

After conferring with a number of materials experts, the author concluded that the approach with the greatest chance of success consisted of mechanically bonding flanged ceramic sections with ceramic bolts and graphite foil gaskets.

The bolts, machined from the same material as the solar receiver, would have the same CTE as the main body[**] and should neither fracture the flange (in compression) or open it to leakage (in tension).

Figure 8. Solar receiver and graphite foil (Grafoil) gaskets.

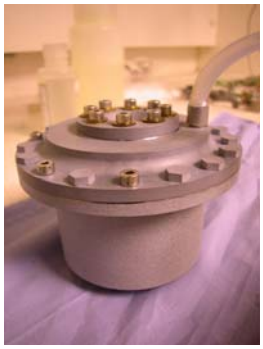

Figure 9. Sealed solar receiver undergoing 3.9 bar leak check.

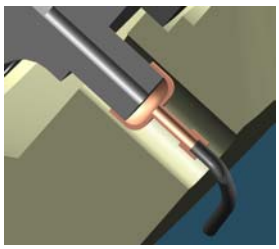

Figure 10. Cavity receiver feedline detail.

Figure 11. Braze test configuration.

Figures 7 and 8 illustrate the mechanical bonding scheme used in the construction of the solar receiver. Figure 9 shows the assembled receiver fitted with a silicone line for leak testing. The author was able to achieve approximately 4 bar of internal pressure under ambient conditions without any leakage around the three graphite seals. There was some apparent leakage around the heads of several bolts; during assembly, it was found that the IMC bolts (4-mm diameter) would fracture at torque levels of between 0.2 and 0.4 N-m, making it difficult to fully tighten the bolts onto the flange faces.[††] Despite this, however, the approach appears successful. Further tests will validate the mechanical bonding scheme at elevated temperatures and full flow, in vacuum. Introducing propellant into the solar receiver necessitates a ceramic-to-metal joint capable of withstanding very high temperatures (Fig. 10).

[**] For IMC, this figure is 7.0 x 10^{-6} in/in/°C. This is slightly higher than two key refractory metals, tungsten (4.5 x 10^{-6}) and molybdenum (5.1 x 10^{-6}).

[††] This has been resolved by the procurement of molybdenum bolts and nuts, which should expand less than the IMC flange material, holding the vessel together in compression at operating temperatures.

The author selected molybdenum as the feedline material, given its workability, relatively low cost, and refractoriness. Molybdenum's melting point is 2,883 K.

Options for joining molybdenum to TiB_2/BN include mechanical assembly (e.g., bolted flanges or screw fittings), high-temperature adhesives, and brazing. All of these approaches—and some combinations thereof—are being investigated. Gasketed screw fittings have been designed and will be delivered in late spring. Several ceramic adhesives with use temperatures of up to 2,033 K have been ordered.

Potential braze filler materials were investigated, and two selected for further examination: eutectic molybdenum/ruthenium (Mo/Ru) and a mixture of pure Mo, silicon, and molybdenum disilicide.[20] This second approach, suggested by B. Derby of the Manchester Materials Science Institute, is an example of partial transient liquid phase bonding (PTLPB), potentially creating a high-temperature solid phase intermediate between the ceramic and metal surfaces. Mo/Ru, with a melting point of 2,320 K, was successfully used to bond single-crystal molybdenum solar receiver elements in a Japanese test programme conducted in the late 1990s.[21] While there was no specific evidence in the literature that suggested that such a bond would be achievable, eutectic Mo/Ru represented just one of a very few non-proprietary refractory metal brazes available.[22] It was believed that long experience with molybdenum/manganese metallisation of ceramic elements, might make such a bond feasible.[23]

Figure 12. Braze test specimen, Mo/Ru filler, Mo cap, IMC post. Pressure < 10^{-4} mbar.

Figure 13. Braze test specimen, Mo/Ru filler, Mo cap, IMC post. Pressure = 1-2 mbar.

In vacuum and low pressure tests at the University of Manchester in March 2003, the author was able to achieve a non-hermetic bond between a molybdenum cap and a test post

composed of IMC ceramic (Fig. 11).[‡‡] Peak furnace temperature attained was 2,060 K, short of the eutectic by several hundred degrees; pressure levels were maintained below 10^{-4} mbar (Fig. 12). A very weak bond was achieved at 2,073 K at a pressure of 1-2 mbar, with clear evidence of oxidation (Fig. 13). In both cases, the braze filler material clearly wet the metal cap but refused to flow freely over the ceramic.

An attempt was made to improve the seal quality of the Mo/Ru bond at temperatures approaching the braze filler liquidus of 2,320 K. This effort has so far proved unsuccessful, owing to the unexpected melting of the Mo cap. The author has conferred with various experts on probable causes of the premature melt—to include melting point suppression by elemental boron migration, infiltration of molybdenum grain boundaries by titanium, and the potential inclusion of impurities in the cap material itself—but no conclusion has yet been drawn.

Further braze tests will be conducted through the summer. A combination of brazing (to ensure high bond strength) and application of ceramic adhesive (to ensure hermeticity) is thought to be the most promising current approach.

Optical Modelling and Test

The insulated cavity receiver shown in Figure 3 behaves as a near-perfect blackbody with an emissivity approaching unity. To minimise heat loss from the body, both low thermal conductivity insulation and a small optical aperture are required. At 2,500 K, a 12 mm diameter aperture will radiate approximately 250 W to space. Given that the 56-cm mirror fabricated for this effort is only capable of generating about 270 W, and that there are other sources of heat loss in the system—to include radiative losses from the insulation surface and conductive losses along the feedline and structural supports, it is clear that the smallest achievable aperture—and thus the highest concentration ratio,[§§] is needed. Hottel[24] has shown that the maximum concentration ratio (C_{max}) of a parabolic point-focus mirror is:

$$C_{max} = \frac{1}{\sin^2\theta_{sun}},$$

where θ_{sun} is the solar half-angle, which is approximately 0.25° at the nominal earth-sun separation. This theoretical maximum (~52,000) is not normally achievable in practice; Kreider provides a relation for flat-plate receivers which results in a maximum C of 13,000.[25]

Figure 14. 56-cm aluminium concentrating mirror on diamond turning tool following fabrication.

The 56-cm, 15-kg aluminium mirror (Fig. 14) is an uncoated, diamond-turned optic procured from Precision-Optical Engineering (P-OE) in Hitchin, Hertfordshire, UK. It is a fast (fractional f-number) mirror with a rim angle of 45°, a focal length of 33.7 cm, and an areal density of approximately 60 kg/m^2—slightly heavier than the solid model estimate. Designed for maximum concentration, it should theoretically produce a solar image at the focal plane of 4.9 mm diameter.

P-OE provided interferogram and form error data for the central portion of the concentrator but was unable to sample a full diameter. This data indicated that the mirror's surface never deviates more than 1.25 microns (1250 nm) from an ideal paraboloid (Fig. 15). A rough estimate of the mirror's RMS wavefront error can be determined; it is found to be approximately 1.34 microns.[***]
Using the ray-trace software package OSLO LT, the author was able to demonstrate that this level of optical performance, while inadequate for optical imaging, is more than sufficient to produce concentration ratios of 10,000 or

[‡‡] Attempts to bond a molybdenum cap to ZSBN using the Mo/$MoSi_2$/Si PTLPB approach at temperatures of up to 2,052 K were unsuccessful.

[§§] A geometric concentration ratio (C_g) is simply the intercepted area of the solar collector divided by the focal spot (solar image) size. A more useful definition of concentration ratio (C) is based on heat flux; in this instance, the solar flux incident on the collector is divided by the heat flux incident on the receiver aperture. The author's target value of C is 10,000.

[***] This is insufficient to produce diffraction-limited images, which generally requires "quarter-wave" (160 nm) or better RMS wavefront error.

greater. A form error profile approximating P-OE's test data gives a spot size of almost precisely 5 mm, while a similar error profile (but with an RMS form error of almost 60 microns) gives a spot nearly 10 mm in diameter (Fig. 16). A doubling of spot size reduces effective concentration by a factor of four; thus, a mirror with 60 microns of form error can do no better than a concentration ratio of 3,250.

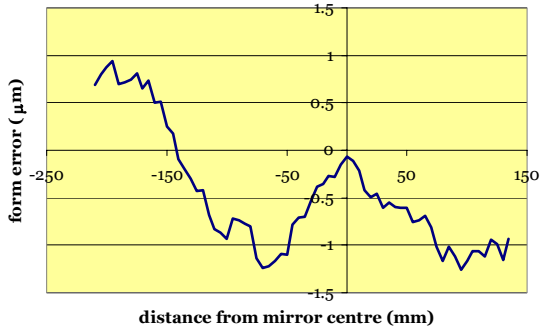

Figure 15. 56-cm mirror form error (sag) data.

The 60-micron figure sets a limit to acceptable form error and clearly permits composite mirrors to achieve concentration ratios of the order required.

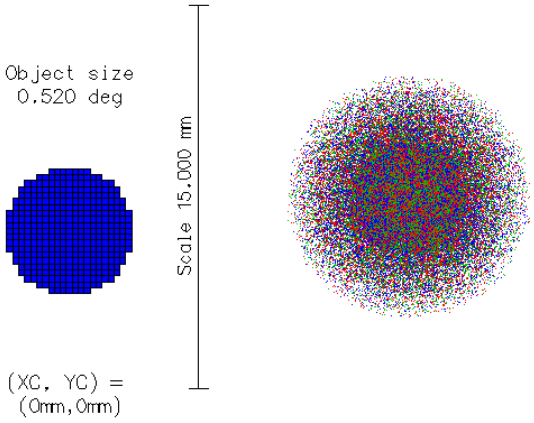

Figure 16. 9.5 mm spot size resulting from 60 micron form error in 56-cm, f/.60 concentrator.

In early May 2003, the concentrating mirror was mounted on a Losmandy GM-11 German Equatorial telescope mount to facilitate precise solar tracking. A Kipp & Zonen CH-1 pyrheliometer, which measures incident solar flux, was mounted to the mirror support. A small, shielded spotting scope with an electronic eyepiece was also attached to the support structure, in order to ascertain mirror alignment. Initial tests were conducted to measure solar image size at the focal plane; a cooled copper target engraved with concentric rings was mounted at the focus to allow the measurement to take place (Fig. 17).

Figure 17. Optical test rig mounted on Losmandy GM-11 mount.

Photographs of the copper target during on-sun testing confirmed that the diameter of the spot is slightly less than 5 mm (Fig. 18), which implies a C_g of more than 12,500. However, non-unity mirror reflectance and imperfect specularity could reduce the heat flux delivered to the spot, despite its apparent size. This would result in a smaller value of *C*.

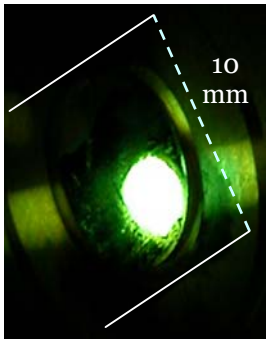

Figure 18. Photograph of centre of copper target during on-sun testing.

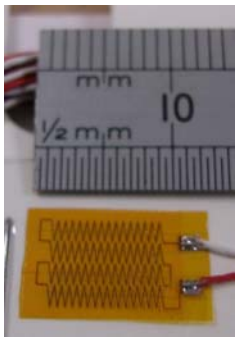

Figure 19. RdF micro-foil heat flux sensor, Type 27133-1, 50 W/cm² maximum.[26]

An RdF heat flux sensor (Fig. 19) rated to 50 W/cm² was mounted on the copper target and the mirror exposed to direct sunlight for several seconds. The sensor reported heat flux values of up to 33 W/cm² before failing. Since expected heat flux values at the target range between 500 and 1,000 W/cm², this failure was not unexpected.

As an alternative to direct measurement, the author conducted a second on-sun test while measuring bulk copper target temperature. A C-type (tungsten/rhenium) thermocouple used for cavity receiver testing was inserted into the interior of the target, with its bead placed directly behind the focal point. After an equilibrium temperature was reached, the

mirror was covered and temperature data was recorded (Fig. 20). In the case of a body where internal conduction is irrelevant and its surface temperature (T) is approximately equal to its bulk temperature,

$$\frac{dT}{dt} = \frac{Q}{\rho C_p V}.$$

Here, $\rho C_p V$ is the target's heat capacity in joules (J). Instantaneously following the covering of the mirror, heat loss from the target will be essentially equivalent to the heat flux falling on the target just prior to the shutoff. This loss was calculated using temperatures at both shutoff and 30 seconds afterwards. The 120-minute test, conducted at an average solar flux of 742 W/m², resulted in (1) an intercepted flux of 183 W at the mirror, and (2) a heat flux figure at the target of 147 W, or roughly 750 W/cm². This gives an effective concentration ratio of 10,072—in line with the stated requirement of 10,000.

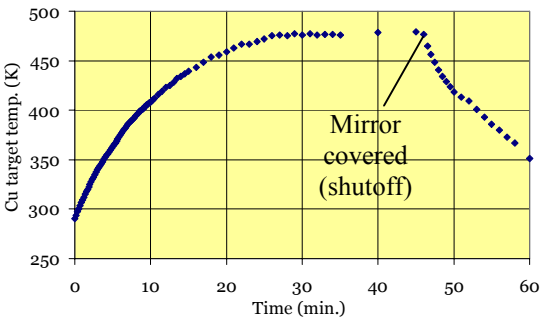

Figure 20. Copper target temperature as function of time.

Further optical testing will be performed to investigate off-nominal concentrator performance, including focal length offsets and pointing inaccuracies. Following this characterization, the solar receiver will be tested on-sun to ascertain differences between the electrical and incident solar heating cases.

Thermal Modelling and Test

Initial thermal modelling by the author included one-dimensional simulations of a cylindrically symmetric solar receiver and insulation package.[27] Further refinement of these results required the use of Thermoanalytics, Inc., multi-mode heat transfer software WinTherm 7.0.[†††]

[†††] WinTherm uses an implicit Crank-Nicholson finite difference scheme to simultaneously solve for radiation, conduction, and convection. Models in WinTherm are constructed from shell, rather than solid, elements; temperature profile data within shell elements is limited to the shell's two external surfaces and two internal interfaces.

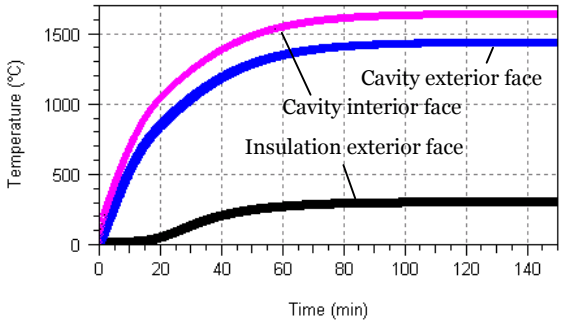

Figure 21. Solar receiver with 500 W radiative input, insulation package k = 0.12 W/m-K.

Figure 21 depicts typical output for a 500-W heating case. After 70 minutes, the internal (hot face) surface of the cavity has risen to over 1,600° C (1,873 K), while the exterior (insulation facing) surface is some 200 degrees cooler. Model assumptions include aperture size, thermal conductivity, emissivity, and specific heat values for the receiver structure, particle bed, and insulation package. At lower flux levels, peak temperature declines significantly (Fig. 22): A 325-W input reaches equilibrium at only 1,145° C (1,418 K).[‡‡‡] These figures indicate substantially greater heat losses than the initial models suggest.

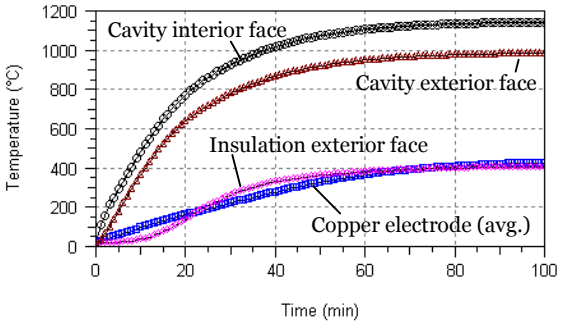

Figure 22. Solar receiver, 325 W radiative input, insulation k = 0.25 W/m-K. The electrical heating apparatus is included in the model.

The first tests of the insulated solar receiver concentrated on the validation of WinTherm modelling results for the thermal charging phase. The receiver was placed in its insulation package (Fig. 23) and suspended between two aluminium mounting rings, then placed inside a small vacuum chamber fitted with power, thermocouple, and pressure measurement leads

[‡‡‡] The insulation package's thermal conductivity was revised upwards to correspond with results seen in actual testing. The vendor's stated value is 0.12 W/m-K.

(Fig. 24). A combination of rotary and oil diffusion pumps permitted pressures of less than 10^{-4} mbar to be attained after approximately 45 minutes.

Figure 23. Solar receiver in graphite insulation package (cap section removed).

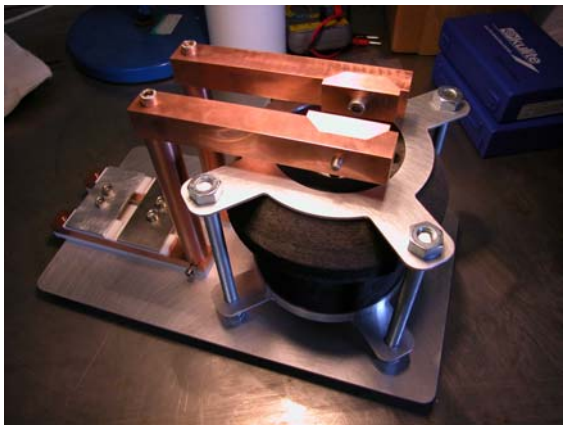

Figure 24. Solar receiver heating test rig. Copper electrodes are suspended over the receiver aperture; the heating element is clamped between the electrodes and inserted inside the cavity.

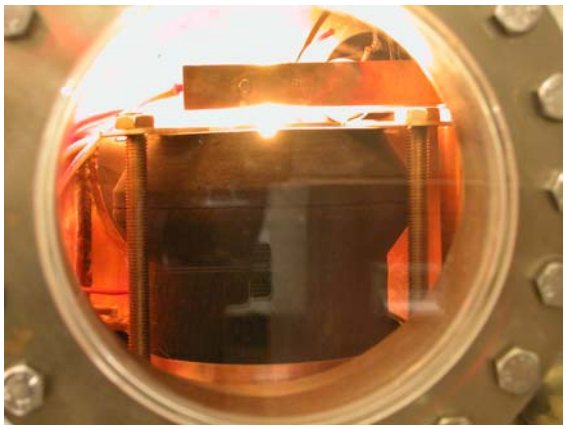

Figure 25. Solar receiver undergoing electrical heating in vacuum.

Solar flux was simulated through the use of radiative elements suspended inside the receiver cavity. Several factors combined to make electrical heating of the cavity somewhat difficult: (1) volumetric constraints and small aperture diameter (8 mm); (2) IMC's natural conductivity, which requires the heating elements to be separated from the cavity walls; and (3) deterioration of heating element material in vacuum, through vaporisation, leading to element failure. Both tungsten wire coils (of varying diameter, 0.25-1.0 mm) and IMC rods were used to heat the receiver.

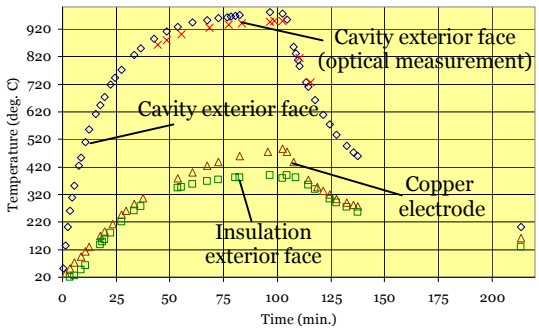

Figure 26. Insulated cavity receiver electrical heating test, 16 April 2003. Peak external cavity temperature achieved: 1,250 K.§§§ Electrical power applied: 872 W.

Despite these difficulties, a number of tests have been conducted at power levels of up to 1,200 W (Fig. 25). This figure represents the total power dissipated in the electrical circuit; to date, no test has resulted in more than 325 W radiative power incident on the solar receiver. The results of one such test, performed in April 2003, are shown in Fig. 26. The results show good agreement with the WinTherm output shown in Figure 22, which incorporates conductive and radiative losses totalling over 500 W. There is evidence of substantial conductive loss to the copper electrodes, which were heated to over 750 K in this test. Efforts have been made since this test to improve the efficiency of the heating elements by depositing the greater portion of generated heat inside the cavity. The author expects to be able to test at radiated powers of 400 to 1,000 W over the next several months. This will determine the actual power needed to heat the solar receiver to projected use temperatures (2,000-2,500 K) and thus provide a definitive estimate of the concentrating mirror size required.****

While the *Mk. I* receiver was initially designed to provide ~400 N-s of impulse per firing,

§§§ Peak internal cavity temperature was not recorded, owing to the difficulty of thermocouple placement and infrared thermometer viewing.

**** It appears likely that the power required to heat the *Mk. I* receiver will be on the order of 600-750 W, necessitating a mirror diameter of 75 cm or greater.

machinability concerns increased flange thicknesses and added substantially to receiver mass. The *Mk. I* receiver, as built, is approximately equivalent in mass and thermal capacity to the 750 N-s receiver discussed earlier in this paper. A *Mk. II* receiver, lighter in weight and possessing a thicker insulation package, will be constructed later this year.

Future Testing

The principal focus of the current effort is to complete the electrical heating tests of the *Mk. I* solar receiver. Once this is concluded, the author will proceed with flow testing in vacuum, using N_2, H_2, inert gas, and ammonia propellants. The purpose of these tests is threefold:

1. To verify estimates of the cavity receiver's heat transfer coefficient;

2. To prove out the engine's ability to withstand repeated attack by selected propellants and their analogues; and

3. To provide an estimate of the engine's burn-average I_{sp} and thrust.

Seal and bonding tests are continuing. A second solar receiver will be assembled with molybdenum fasteners and tested at pressures of between 8 and 20 bar. Mo/Ru brazing, which appears capable of providing high-strength bonds between IMC and molybdenum metal, will be further investigated, both by itself and in conjunction with high-temperature ceramic adhesives to promote hermetic seals. Gasketed screw-fit feedline caps will also be examined for their efficacy.

On-sun characterization of the aluminium concentrator continues. The author will examine the sensitivity of the system to errors in solar tracking and focal length. Further tests will integrate the concentrator and receiver subsystems in order to ascertain differences in outcome between electrical and direct solar heating of the cavity receiver. On the basis of these and other tests, a smaller *Mk. II* receiver will be built to better match the light gathering power of the 56-cm mirror.

Summary and Conclusions

Over the past year, the author has designed, fabricated, and tested several critical elements of the microscale STP system. These include:

1. The validation of a low-cost solar receiver design composed of uncoated ceramic elements, bonded mechanically and gasketed with high-temperature graphite foil to maintain hermeticity, with materials capable of surviving temperatures in excess of 2,300 K;

2. Confirmation of the utility of refractory metal brazes, enabling ceramic-to-metal bonding between molybdenum and non-reactive nitride ceramic composites;

3. The fabrication and successful testing of a low-cost aluminium concentrating mirror, at concentration ratios of greater than 10,000, closely agreeing with model results; and

4. Low-power electrical testing of the assembled solar receiver in a simulated environment, demonstrating good agreement with thermal models, at peak temperatures of 1,400-1,500 K.

Further attempts will be made to duplicate Mo/Ru bonding between Mo and IMC elements. Hybrid braze/adhesive approaches will be examined for their utility in providing a strong, hermetic bond between receiver and feedline elements. Additional concentrating mirror tests will examine performance in off-nominal cases, including tracking and focal length inaccuracies. Full flow receiver characterization tests are slated for this summer, at temperatures of up to 2,000 K, with a number of propellants.

Lessons learned from this test campaign will be use to refine the design of a smaller, lighter weight solar receiver, the *Mk. II*. This receiver will be tested later in the fall of 2003.

Acknowledgements

The author would like to thank Patrick Frye of Boeing's Rocketdyne Division, who has supplied indispensable moral and financial support; Bill Marinelli; Dr. Stu Nozette; Dr. Julie Yeomans and Prof. John Watts of the University of Surrey's Materials Science Department; Andy Blackburn of MAST Carbon; Prof. Brian Derby and Dr. Andrew Winn of the Manchester Materials Science Centre; Dr. Ian Coxhill and Dr. Adam Baker; David Gibbon; and Malcolm Paul, whose unflagging support made a sometimes difficult test campaign run smoothly.

References

1. "First DMC Microsatellite Releases Imagery," http://www.sstl.co.uk/news.html, Surrey Satellite Technologies, Ltd., Nice, A., Guildford, United Kingdom, 2 April 2003.

2. *Space Propulsion Analysis and Design,* McGraw-Hill, New York, Humble, R., Henry, G., and Larson, W., 1995.
3. *Investigation into Low-Cost Propulsion Systems for Small Satellite Missions,* Sellers, J., Ph.D. thesis, Department of Electrical Engineering, University of Surrey, Guildford, UK, June 1996.
4. *Research into Resistojet Rockets for Small Satellite Applications,* Lawrence, T., Ph.D. thesis, University of Surrey, Guildford, UK, 1998.
5. *Alternative Geometry Hybrid Rockets for Spacecraft Orbit Transfer,* Haag, G., Ph.D. thesis, University of Surrey, Guildford, UK, 2001.
6. "An Investigation of a Low Cost HTP/Kerosene 40 N Thruster for Small Satellites," Coxhill, I., Richardson, G., and Sweeting, M., Proceedings of the 38th Joint Propulsion Conference, Indianapolis, Indiana, July 2002.
7. "Nitrous Oxide as a Rocket Propellant," Zakirov, V., and Sweeting, M., Lawrence, T., and Sellers, J., *Acta Astronautica* **48**, *No. 5-12, pp. 353-362*, Surrey Space Centre and the European Office of Aerospace Research and Development, 2001.
8. "Preliminary Design of a Micro-Scale Solar Thermal Propulsion System," Kennedy, F., and Palmer, P., AIAA 2002-3928, 38th Joint Propulsion Conference, Indianapolis, Indiana, July 2002.
9. "European Activities in Electric Propulsion," Proceedings of the 3rd International Conference on Spacecraft Propulsion, pp. 49-63, ESA SP-465, Saccocia, G., Cannes, France, December 2000.
10. LunarSat: The Mission, http://www.lunarsat.de/, web page, 2002.
11. "Surrey Platforms: GEMINI Direct," Surrey Satellite Technologies, Ltd., (SSTL), http://www.sstl.co.uk/datasheets/Platform_GEMINI_HQ.pdf, web page, Guildford, UK, 1999.
12. "Minimising the Size and Mass of Interplanetary Spacecraft," 52nd International Astronautical Congress, Toulouse, France, Wells, N., and Fearn, D., Space Department, QinetiQ, October 2001.
13. Ariane Structure for Auxiliary Payload 5 User's Manual, Issue 1, Rev. 0, Mugnier, D., Arianespace, Evry, France, May 2000.
14. "A Critical Review of Ultralightweight Composite Mirror Technology," Kasl, E., Crowe, D., Proceedings of the Conference on Advanced Materials for Optics and Precision Structures, San Diego, California, Composite Optics, July 1997.
15. "Composite Optics, Inc., Successfully Completes the World's Largest, Lightest Weight, Composite Mirror," Composite Optics, Inc., http://www.coi-world.com/first.htm, web page, San Diego, California, August 2000.
16. "Boron Nitride," St. Gobain Advanced Ceramics, Amherst, New York, company brochure with technical data, November 2000.
17. "Titanium Diboride/Boron Nitride, Intermetallic Composite Powder Material Safety Data Sheet (MSDS)," GE Advanced Ceramics, http://www.advceramics.com/acc/downloads/, web page, Cleveland, Ohio, 12 April 2000.
18. *Handbook of Refractory Carbides and Nitrides,* Pierson, H., Noyes Publications, Westwood, New Jersey, 1996.
19. "Some Observations on the Wetting and Bonding of Nitride Ceramics," Nicholas, D., Mortimer, L., *J. Mat Sci.* ***25****, No. 6*, 1990.
20. *Binary Alloy Phase Diagrams, Vol. 2,* T. Massalski, ed., American Society for Metals, Metals Park, Ohio, 1986.
21. "Fabrication and Testing of Single Crystal Mo Solar Thermal Thruster," 48th International Astronautical Congress, Shimizu, M., Itoh, K., and Sato, H., National Aerospace Laboratory (NAL), National Research Institute of Metals (NRIM), and Tokyo Tungsten Co., Ltd., Turin, Italy, October 1997.
22. "Rembar Technical Data," The Rembar Co., Inc., http://www.rembar.com/tech2.htm, web page, Dobbs Ferry, New York, March 2003.
23. *Joining Processes: Introduction to Brazing and Diffusion Bonding,* pp. 28-29, Nicholas, M., Kluwer Academic Publishers, Dordrecht, The Netherlands, 1998.
24. *Radiative Transfer,* Hottel, H., and Sarofim, A., McGraw-Hill, 1967.
25. *Medium and High Temperature Solar Processes,* Kreider, J., Academic Press, New York, 1979.
26. "RdF Heat Flux Sensors," RdF Corporation, http://www.rdfcorp.com/products/hflux/hfs-a_03.shtml, web page, Hudson, New Hampshire, March 2003.
27. "Design and Proto-Flight Test Strategy for a Microscale Solar Thermal Engine," Kennedy, F., and Palmer, P., IAF-02-S.6.05, 53rd International Astronautical Congress, Houston, Texas, October 2002.

The views expressed in this article are those of the author and do not reflect the official policy or position of the United States Air Force, Department of Defense, or the U.S. Government.